

LATERITIN, A NEW INHIBITOR OF ACYL-CoA:CHOLESTEROL  
ACYLTRANSFERASE PRODUCED BY *Gibberella lateritium* IFO 7188

KEIJI HASUMI, CHIKARA SHINOHARA, TAKASHI IWANAGA and AKIRA ENDO\*

Department of Applied Biological Science, Tokyo Noko University,  
3-5-8 Saiwaicho, Fuchu, Tokyo 183, Japan

(Received for publication June 24, 1993)

A new inhibitor of acyl-CoA:cholesterol acyltransferase (ACAT), designated lateritin, was isolated from the mycelial cake of *Gibberella lateritium* IFO 7188 by successive purification procedure of solvent extraction, silica gel column chromatography and reverse phase HPLC. Spectroscopic analyses of the compound yielded 4-methyl-6-(1-methylethyl)-3-phenylmethyl-1,4-perhydrooxazine-2,5-dione as the proposed structure. Lateritin inhibited rat liver ACAT activity by 50% at a concentration of 5.7  $\mu\text{M}$ . This inhibition was time-dependent and irreversible.

The existence of macrophage-derived foam cells loaded with a large amount of esterified cholesterol is a prominent feature of the early lesion of atherosclerosis. These cholesteryl esters are synthesized from fatty acyl-CoA and cholesterol by the enzyme acyl-CoA:cholesterol acyltransferase (ACAT)<sup>1</sup>. In the course of searching for the inhibitors of cholesteryl ester formation in macrophages, we found several compounds, including acaterin as an inhibitor of ACAT<sup>2</sup>. Further search led to the isolation of a new ACAT inhibitor, lateritin (Fig. 1), from *Gibberella lateritium* IFO 7188. The present paper deals with the isolation, characterization and biological activity of lateritin.

#### Fermentation

For the maximal production of lateritin, *G. lateritium* IFO 7188, obtained from the Institute for Fermentation, Osaka, Japan, was grown in Sakaguchi flasks at 25°C for 3 days using the medium containing 3% glucose, 1% soybean meal, 0.3% meat extract, 0.3% polypeptone, 0.3% yeast extract, 0.05%  $\text{KH}_2\text{PO}_4$ , 0.05%  $\text{MgSO}_4 \cdot 7\text{H}_2\text{O}$  and 0.01% CB442 (an antifoam, Nippon Oil & Fat Co., Tokyo, Japan). A typical time course of the fermentation is shown in Fig. 2, where the production of lateritin

Fig. 2. Time course of the production of lateritin.  
(□) pH, (○) lateritin.

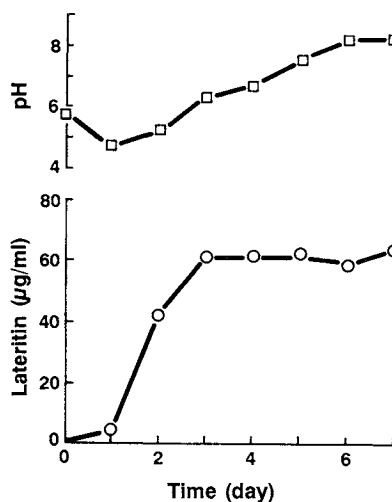
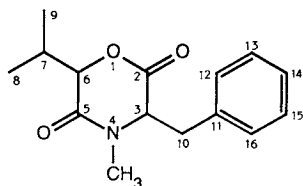


Fig. 1. The structure of lateritin.



*G. lateritium* IFO 7188 was grown at 25°C in a 500-ml Sakaguchi flask containing 100 ml of the medium by shaking at 120 strokes/minute.

was monitored by HPLC analysis of the acetone extract of the mycelial cake.

#### Isolation

The mycelial cake obtained from 2.4 liters of the cultured broth was washed with water and extracted with three 700 ml portions of acetone. The acetone extract was concentrated to about 100 ml and extracted with three 100 ml portions of dichloromethane at pH 3. The solvent layer was dried over sodium sulfate and concentrated to dryness, giving 460 mg of an oily residue. This material was applied to a silica gel column (15 × 140 mm, Wakogel C-200). After washing with *n*-hexane-acetone (9:1), the column was developed with 460 ml of *n*-hexane-acetone (4:1). The active fractions were combined and concentrated to dryness, giving 110 mg of an oily residue. The residue was dissolved in methanol and subjected to preparative HPLC using an Inertsil PREP-ODS column (20 × 250 mm, GL Sciences, Tokyo, Japan). The column was developed with acetonitrile-water (7:3) and the active fractions were combined and extracted with dichloromethane at pH 3 after removing acetonitrile by evaporation. The dichloromethane extract was dried over sodium sulfate and concentrated to dryness to give 48 mg of purified lateritin. The purity of lateritin was examined by a combination of chromatographic (TLC and HPLC) methods. The conditions of TLC and HPLC were: TLC, R<sub>f</sub> 0.61 in a solvent system of *n*-hexane-acetone (1:1) on a silica gel plate (Kieselgel 60 F<sub>254</sub>, E. Merck, Darmstadt, Germany); HPLC, retention time 17.5 minutes on a Inertsil PREP-ODS column, 6 × 250 mm, GL Sciences, developed with acetonitrile-water (7:3) at a rate of 2 ml/minute at 40°C and detected by UV absorption at 200~280 nm using a photodiode array detector.

#### Physico-chemical Properties and Structure

##### Elucidation

Lateritin was obtained as a light brown oil. The physico-chemical properties of lateritin are summarized in Table 1. Its IR spectrum is shown in

Table 1. Physico-chemical properties of lateritin.

Appearance	Light brown oil
Molecular formula	C <sub>15</sub> H <sub>19</sub> NO <sub>3</sub>
SI-MS ( <i>m/z</i> )	262 (M+H) <sup>+</sup>
HREI-MS ( <i>m/z</i> )	
Calcd:	261.1365 for C <sub>15</sub> H <sub>19</sub> NO <sub>3</sub>
Found:	261.1275 (M) <sup>+</sup>
UV λ <sub>max</sub> <sup>EtOH</sup> nm (ε)	202 (8,390), 258 (228)
IR ν <sub>max</sub> (KBr) cm <sup>-1</sup>	2955, 2923, 2865, 1738, 1652, 1364, 1174, 1100, 1054, 1012

Fig. 3. IR spectrum of lateritin (KBr).

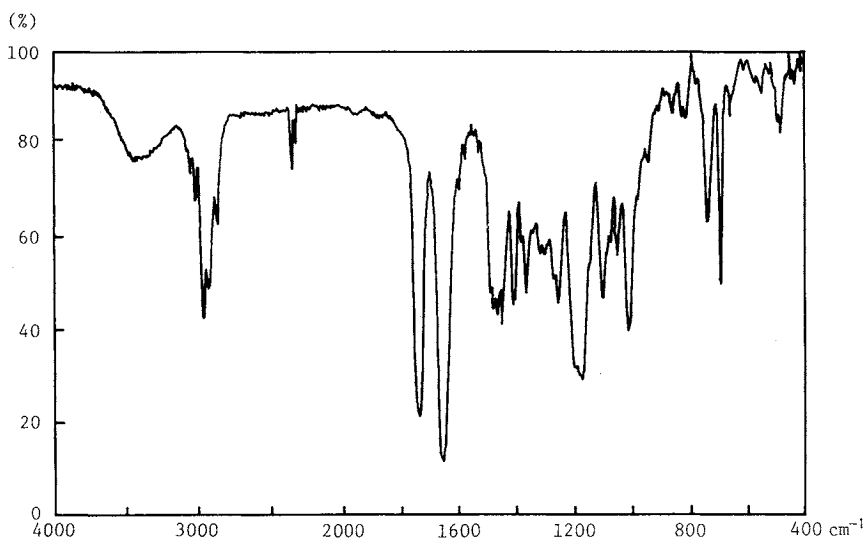


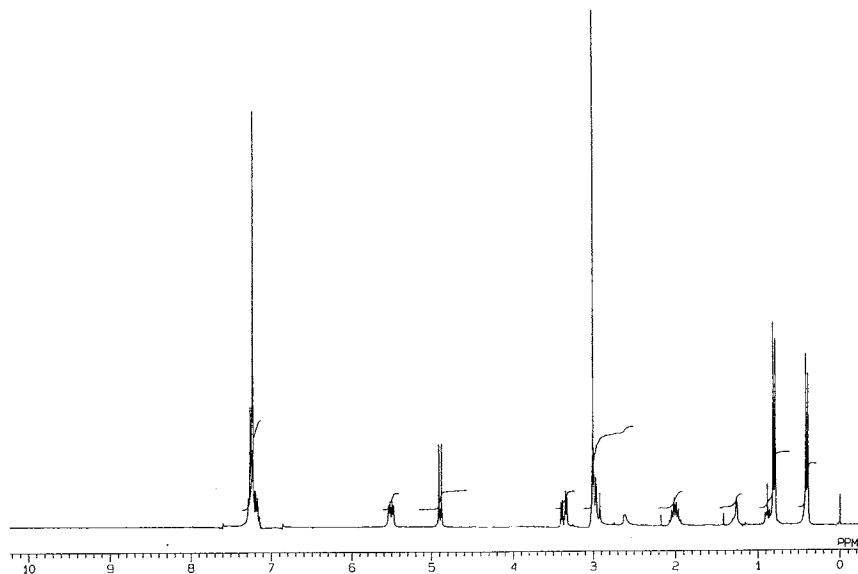
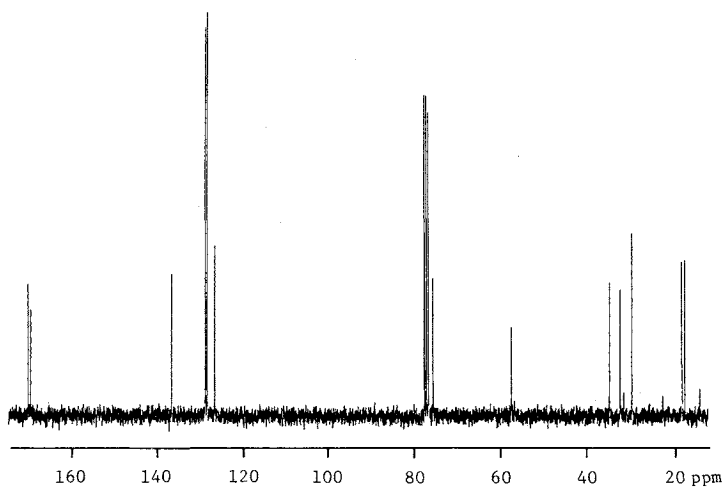
Fig. 4.  $^1\text{H}$  NMR spectrum of lateritin ( $\text{CDCl}_3$ , 270 MHz).Fig. 5.  $^{13}\text{C}$  NMR spectrum of lateritin ( $\text{CDCl}_3$ , 67.9 MHz).

Fig. 3, and  $^1\text{H}$  and  $^{13}\text{C}$  NMR spectra in Figs. 4 and 5, respectively. The data from SI-MS, HREI-MS and  $^{13}\text{C}$  NMR analyses of lateritin established  $\text{C}_{15}\text{H}_{19}\text{NO}_3$  as its molecular formula. The  $^1\text{H}$  NMR,  $^{13}\text{C}$  NMR (complete decoupling and DEPT) and  $^{13}\text{C}$ - $^1\text{H}$  COSY spectra of lateritin revealed the presence of three methyl, one methylene, one aliphatic methine, five aromatic methine, one aromatic quaternary and two carbonyl carbon atoms as well as two methine carbon atoms bearing polar substituents (summarized in Table 2). The signals of five methine carbons ( $\delta_{\text{C}}$  126.74, 128.51 and 128.88) and one quaternary carbon ( $\delta_{\text{C}}$  136.65) in the NMR spectra suggested the presence of a phenyl group. The *geminal*-coupled methylene protons at  $\delta_{\text{H}}$  2.97 and 3.38 ( $J=14.5$  Hz) showed spin couplings with the proton of *N*-linked methine at  $\delta_{\text{H}}$  5.51 ( $J=4.8$  and 11.8 Hz). Spin couplings were also observed between two methyl signals ( $\delta_{\text{H}}$  0.41,

Table 2.  $^1\text{H}$  and  $^{13}\text{C}$  NMR data for lateritin.

Position	$\delta_{\text{C}}$ (67.9 MHz)	$\delta_{\text{H}}$ (270 MHz)
2	169.90	—
3	57.34	5.51 (1H, dd, $J=4.8, 11.8$ )
4- $\text{CH}_3$	32.34	2.99 (3H, s)
5	169.34	—
6	75.46	4.89 (1H, d, $J=8.43$ )
7	29.68	1.99 (1H, m)
8	17.47	0.41 (3H, d, $J=6.60$ )
9	18.26	0.85 (3H, d, $J=6.96$ )
10	34.75	2.97 (1H, dd, $J=11.8, 14.5$ ), 3.38 (1H, dd, $J=4.8, 14.5$ )
11	136.65	—
12, 16	128.88	7.2 (1H, m)
13, 15	128.51	7.2 (1H, m)
14	126.74	7.2 (1H, m)

Spectra were measured in  $\text{CDCl}_3$  at  $25^\circ\text{C}$ . TMS was used as an internal reference ( $\delta$  0.00).  $J=\text{Hz}$ .

$J=6.60\text{ Hz}$  and  $\delta_{\text{H}} 0.85$ ,  $J=6.96\text{ Hz}$ ) and one methine signal at  $\delta_{\text{H}} 1.99$ , which in turn coupled with the signal of oxygen-bearing methine at  $\delta_{\text{H}} 4.89$  ( $J=8.43\text{ Hz}$ ). These results showed the presence of two partial structures,  $-\text{CH}_2-\text{CH}-\text{N}<$  and  $(\text{CH}_3)_2\text{CH}-\text{CH}-\text{O}-$ . From the HMBC and COLOC data, the *geminal*-coupled methylene protons at  $\delta_{\text{H}} 2.97$  and  $3.38$  showed long-range couplings between the aromatic carbons at  $\delta_{\text{C}} 136.65$  and  $128.88$  (Fig. 6). The long-range couplings were also observed between the methine signal at  $\delta_{\text{H}} 5.51$  and the carbon signals at  $\delta_{\text{C}} 136.65$  and  $34.75$ . The *N*-methyl proton at  $\delta_{\text{H}} 2.99$  coupled with the carbons at  $\delta_{\text{C}} 57.34$  and  $169.34$ , and the methine proton at  $\delta_{\text{H}} 5.51$  showed couplings with the carbons at  $\delta_{\text{C}} 32.34$  and  $169.34$ . The methine proton at  $\delta_{\text{H}} 4.89$  showed a long-range couplings between the carbonyl carbons at  $\delta_{\text{C}} 169.34$  and  $169.90$ . From these results, it was proposed that the two partial structures are combined to form, through ester and amide bonds, a substituted 1,4-perhydrooxazine ring as shown in Fig. 6. This structure was further confirmed by the analysis of fragment ions in HREI-MS spectrum (Fig. 7). From these observations, the structure of lateritin was established to be 4-methyl-6-(1-methylethyl)-3-phenylmethyl-1,4-perhydrooxazine-2,5-dione as illustrated in Fig. 1.

Fig. 6. Long-range couplings observed in the HMBC and/or COLOC spectra of lateritin.

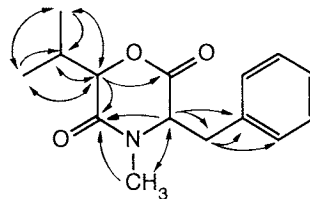
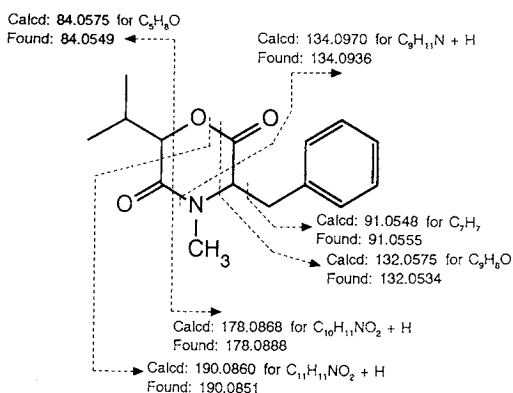


Fig. 7. Mass fragmentation of lateritin.



### Biological Activity

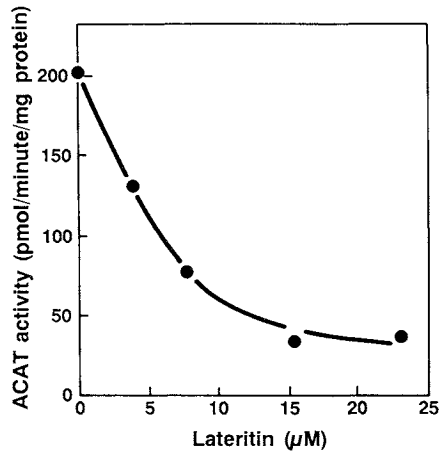
#### ACAT Inhibition

ACAT activity was assayed using microsomes prepared from rat liver as described previously<sup>2)</sup> with slight modifications. As shown in Fig. 8, lateritin inhibited ACAT activity by 50% at a concentration of  $5.7\ \mu\text{M}$ . This inhibition was irreversible and time-dependent. Thus, as shown in Table 3, ACAT activity in microsomes treated with lateritin did not recover from the inhibition even after sequential washing of microsomes by centrifugation. Preincubation of microsomes with lateritin resulted in time-dependent inactivation of ACAT (Fig. 9).

#### Inhibition of Cholesteryl Ester Formation in Macrophages

Macrophages take up and degrade modified lipoproteins such as oxidized low density lipoprotein

Fig. 8. Inhibition of ACAT activity by lateritin.



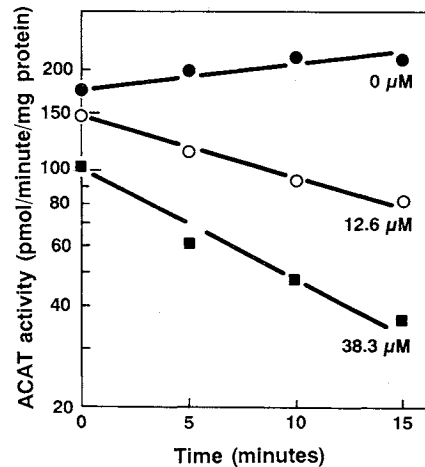
Rat liver microsomes (16.7 mg/ml in 150 mM potassium phosphate, pH 7.4) were preincubated at 37°C for 15 minutes in the presence of the varying concentrations of lateritin. Subsequently, 30 μl of the mixture was added to 20 μl of the mixture containing 150 mM potassium phosphate, pH 7.4, 0.2 mM bovine serum albumin and 0.25 mM [<sup>14</sup>C]oleoyl-CoA (10,000 dpm/nmol) to initiate the enzyme reaction. After incubation at 37°C for 70 seconds, followed by adding 0.25 ml ethanol, cholesteryl [<sup>14</sup>C]oleate formed was extracted with 1 ml of *n*-hexane. The extract was concentrated to dryness and dissolved in 50 μl of *n*-hexane containing 25 μg of cholesteryl oleate as a carrier, and a portion (40 μl) of the sample was submitted to TLC<sup>2)</sup>. The spot of cholesteryl ester was visualized by iodine vapor and their amount was determined by scraping the spot off the chromatogram, followed by scintillation counting. Each value represents the average of duplicate determinations.

Table 3. Irreversible inhibition of ACAT activity by lateritin.

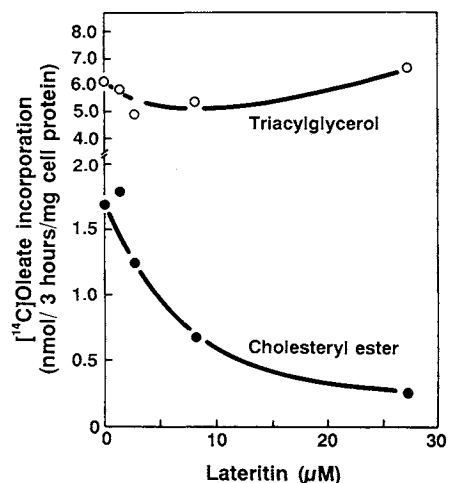
Microsomal washing (frequency)	ACAT activity in microsomes (pmol/minutes)	
	Without lateritin	Lateritin-treated
0	81.0	31.4
1	84.9	28.2
2	77.0	32.1

Rat liver microsomes (16.7 mg/ml in 150 mM potassium phosphate, pH 7.4) were incubated at 37°C for 15 minutes in the presence or absence of 38.3 μM lateritin. Subsequently, aliquots were removed for ACAT assay and remaining portion was washed by ultracentrifugation with buffer containing 150 mM potassium phosphate, pH 7.4, and 80 μM bovine serum albumin as described previously<sup>2)</sup>. ACAT activity was determined as described in the legend to Fig. 8. Each value represents the average of duplicate determinations.

Fig. 9. Time-dependent inhibition of ACAT activity by lateritin.



Rat liver microsomes (16.7 mg/ml in potassium phosphate, pH 7.4) were preincubated with 0 (●), 12.6 (○) or 38.3 μM (■) lateritin at 37°C. At the intervals indicated, ACAT activity was determined as described in the legend to Fig. 8. Each value represents the average of duplicate determinations.

Fig. 10. Effects of lateritin on the incorporation of [<sup>14</sup>C]oleate into cholesteryl ester and triacylglycerol in macrophage J774.

J774 cells were grown as described previously<sup>3)</sup> and received oxidized LDL (100 μg protein/ml) and 0.1 mM [<sup>14</sup>C]oleate (10,000 dpm/nmol) in complex with albumin. After incubation at 37°C for 3 hours in the presence of the indicated concentrations of lateritin, [<sup>14</sup>C]oleate incorporated into cholesteryl ester (●) and triacylglycerol (○) was determined<sup>3)</sup>. Each value represents the average of duplicate determinations.

(LDL), and cholesterol in the lipoprotein is re-esterified in the cells. Treatment of macrophage J774 cells with lateritin resulted in marked inhibition of cholesteryl ester formation as measured by incorporation of [ $^{14}\text{C}$ ]oleate<sup>3)</sup> (Fig. 10). The inhibition was 50% at a concentration of 8.5  $\mu\text{M}$ . Under the same conditions, synthesis of triacylglycerols was not significantly affected. In addition, lateritin also affected neither surface binding, uptake nor degradation of oxidized  $^{125}\text{I}$ -LDL (data not shown).

### Discussion

In the present study, we have isolated a novel substance, designated lateritin, from *G. lateritium* IFO 7188 as an inhibitor of ACAT. Recently, several compounds of microbial origin, including purpactins<sup>4)</sup>, acaterin<sup>2)</sup>, enniatins<sup>5)</sup> and glisoprenins<sup>6)</sup>, have been reported to inhibit ACAT. These compounds inhibit rat liver ACAT by 50% at concentrations ranging from 20 to 120  $\mu\text{M}$ , while  $\text{IC}_{50}$  value of lateritin was about 6  $\mu\text{M}$ . Among these inhibitors of which the inhibition mechanism is disclosed, lateritin is the first irreversible inhibitor of ACAT. Lateritin inhibited cholesteryl ester synthesis from [ $^{14}\text{C}$ ]oleate, whereas it did not affect surface binding, internalization and degradation of oxidized LDL in macrophage J774. Thus, lateritin is a selective inhibitor of cholesterol esterification in the pathway of oxidized LDL metabolism leading to cholesteryl ester formation in macrophages.

### Acknowledgments

The authors are grateful to Dr. J.-T. Woo for helpful comments and discussions. This work was supported in part by a Grant-in-Aid for Science Research from the Ministry of Education, Science and Culture and a Research Grant for Cardiovascular Diseases from the Ministry of Health and Welfare, Japan.

### References

- 1) BROWN, M. S. & J. L. GOLDSTEIN: Lipoprotein metabolism in the macrophage: implications for cholesterol deposition in atherosclerosis. *Annu. Rev. Biochem.* 52: 223~261, 1983
- 2) NAGANUMA, S.; K. SAKAI, K. HASUMI & A. ENDO: Acaterin, a novel inhibitor of acyl-CoA:cholesterol acyltransferase produced by *Pseudomonas* sp. A92. *J. Antibiotics* 45: 1216~1221, 1992
- 3) HASUMI, K.; C. SHINOHARA, S. NAGANUMA & A. ENDO: Inhibition of the uptake of oxidized low density lipoprotein in macrophage J774 by the antibiotic ikarugamycin. *Eur. J. Biochem.* 205: 841~846, 1992
- 4) TOMODA, H.; H. NISHIDA, R. MASUMA, J. CAO, S. OKUDA & S. ŌMURA: Purpactins, new inhibitors of acyl-CoA:cholesterol acyltransferase produced by *Penicillium purpurogenum*. I. Production, isolation and physico-chemical and biological properties. *J. Antibiotics* 44: 136~143, 1991
- 5) TOMODA, H.; H. NISHIDA, X.-H. HUANG, R. MASUMA, Y. K. KIM & S. ŌMURA: New cyclodepsipeptides, enniatins D, E and F produced by *Fusarium* sp. FO-1305. *J. Antibiotics* 45: 1207~1215, 1992
- 6) TOMODA, H.; X.-H. HUANG, H. NISHIDA, R. MASUMA, Y. K. KIM & S. ŌMURA: Glisoprenins, new inhibitors of acyl-CoA:cholesterol acyltransferase produced by *Gliocladium* sp. FO-1513. I. Production, isolation and physico-chemical and biological properties. *J. Antibiotics* 45: 1202~1206, 1992